Desalination and Water Treatment
www.deswater.com
doi: 10.1080/19443994.2014.950991

56 (2015) 1403–1412
October

Taylor & Francis
Taylor & Francis Group

Synthesis of TiO_2/polyacrylonitrile nanofibers composite and its application to lead ions removal from waste waters

Maryam Shojaei[a], Sodeh Sadjadi[b,*], Mehdi Rajabi-Hamane[a], Seyed Javad Ahmadi[b]

[a]*School of Chemical Engineering, College of Engineering, University of Tehran, Tehran, Iran*
[b]*Nuclear Fuel Cycle School, Nuclear Science and Technology Research Institute, End of North Karegar Ave. Po. Box: 14399-51113, Tehran, Iran, email: sadjadi.s.s@gmail.com (S. Sadjadi)*

Received 13 January 2014; Accepted 8 July 2014

ABSTRACT

The adsorption behavior of lead(II) from aqueous solutions utilizing TiO_2/polyacrylonitrile (PAN) nanofibers was studied. TiO_2/PAN nanofibers were prepared by electrospinning method and characterized by X-ray diffraction, Fourier transform infrared spectroscopy, thermogravimetric analysis (TGA), and scanning electron microscope. These data were utilized to show nanofibers and TiO_2 nanoparticles morphology and existence of TiO_2 in nanofibers web. The results show that the size of nanoparticles is about 70 nm and the fibers diameters is in the range of 1–2 μm. The changes in the parameters of adsorbent dosage, pH, contact time, TiO_2 concentration, and temperature were tested in the adsorption experiments. The adsorption was well described by the Langmuir adsorption isotherm model. The thermodynamic parameters indicate that the adsorption process is spontaneous and endothermic. The pseudo-first-order kinetic model describes the dynamic behavior for the adsorption of lead(II) ions onto PAN/TiO_2 nanofibers.

Keywords: Adsorption; Electrospinning; Polyacrylonitrile; Lead(II) ions; Nanofibers

1. Introduction

Heavy metals pollution has become more serious with the rapid increase in global industrial activities. Lead contamination of the environment is among the common global pollutants, has accumulating characteristics in nature and cannot be biodegraded, and this environmental issue is threatening the health of human beings seriously [1,2].

Although the traditional treatment methods such as precipitation, oxidation, reduction, electrochemical treatment, reverse osmosis, solvent extraction, ion exchange, and evaporation can be used for the metal bearing effluents, most of these methods are expensive and difficult to apply [3].

Nanofibers are able to form a highly porous mesh, and their large surface-to-volume ratio improves performance for many applications such as scaffolds in tissue engineering [4], drug delivery systems [5], nanofibrous membranes for fine filtration [6,7], and protective clothing [8]. The utilization of nanofibers is an attractive alternative to traditional separation methods due to their interesting characteristics such as high porosity, large surface area per unit mass, high gas permeability, and small interfibrous pore size [4] which leads to high adsorption rate and capacity as compared to other types of materials such as resins, foams, and conventional fibers [9–11].

*Corresponding author.

1944-3994/1944-3986 © 2014 Balaban Desalination Publications. All rights reserved.

Electrospinning (ES) has the unique ability to produce nanofibers of different materials in various fibrous assemblies. The relatively high production rate and simplicity of the setup makes ES highly attractive to both academia and industry.

In recent years, there has been a growing interest in the incorporation of functional nanoparticles in the polymer nanofibers due to their uniquely promising properties and applications [12–14].

Among these nanoparticles, TiO_2 has received great attention because of its stability, availability, and promise for applications such as painting, catalysis and photocatalysis, battery, cosmetic, in addition, recent studies show great results for adsorption properties of TiO_2 nanoparticles in heavy metals removal from aqueous solutions [15].

Carbon nanofibers have been arousing increased research attention because of numerous advantages such as low density, high aspect ratio, and potential high mechanical, thermal, and electrical performances [16]. About 90% of the carbon fibers produced are made from polyacrylonitrile (PAN). PAN carbon fiber is one of the popular materials that are used in preparing composites for use in commercial aerospace, industrial, space and defense, and electronics markets [17].

In the present study, titanium dioxide (TiO_2) nanoparticles were prepared and dispersed in polymer matrices PAN via ES technique. The nanofibers were subsequently used for the adsorption of lead ions.

2. Experimental

2.1. Apparatus

Crystal structure of the prepared TiO_2 nanoparticles was analyzed by using Cu Kα radiation (Philips PW 1800). Size and morphology of the obtained nanoparticles and nanofibers were observed by scanning electron microscopy (SEM, LEO1455VP). Thermal stability and also chemical compositions of the nanofibers were studied by thermogravimetric analyses (TG-DTA, STA 1500) with heating rate of 10°C/min. IR spectra were recorded with a Brucker Vector 22 spectrometer using KBr disks. Quantitative determinations of inorganic ions were carried out using an inductively coupled plasma-optical emission spectroscope of Varian Turbo Model 150-Axial Liberty.

2.2. Materials

All chemicals were of the highest purity available and were used as received without further purification. PAN (Mw = 150,000), titanium tetraisopropoxide (TTIP or $Ti(O^iPr)_4$, 97%), *N,N*-dimethylformamide (DMF, 99%), oleic acid (OLEA, 99%), and ethylene glycol (EG, 99.8%) were purchased from Sigma-Aldrich. Trimethylamine (TEA, 40% solution in water), methanol, potassium chloride, and lead(II) nitrate were purchased from Merck, AG, Germany.

2.3. Synthesis of TiO_2 Nanoparticles

Ten millimolar of titanium tetraisopropoxide Ti$(O^iPr)_4$ (TTIP) was added to 35 g of OLEA under nitrogen flow at 100°C and allowed to stir for 5 min, giving a pale yellow solution. A 10 mmol of a base trimethylamine ($(CH_3)_3N$ or TMA in 6.4 g of EG was subsequently added. The solution was maintained in a close system and stirred at 100°C over 48 h. The reaction mixture appeared clear during the whole period of the particle growth [18].

TiO_2 nanocrystals were readily precipitated upon addition of an excess of methanol to the reaction mixture at room temperature. The resulting precipitate was isolated by centrifugation and washed twice with ethanol to remove surfactant residuals. The OLEA-coated TiO_2 nanoparticles were then easily redispersed in DMF.

2.4. Preparation of PAN/TiO_2 nanofibers

Fibers of PAN/TiO_2 were obtained by ES. PAN/DMF solution was prepared by dissolving 1 g PAN in 10 mL DMF, and then, 1% (mass fraction with respect to PAN) TiO_2 nanoparticles was added to this solution and has been dispersed by using an ultrasonic apparatus for 2 h. During ES, the applied voltage was held constant at 15 kV, and the distance between the syringe and the collector was kept at 16 cm.

In this study, PAN/TiO_2 nanofibers with different TiO_2 nanoparticle loadings (0.3 and 1%) have been fabricated via a high voltage ES process.

The morphology and size of the resulting ES nonwoven fiber mats and the incorporated nanoparticles were evaluated using SEM, and X-ray diffraction (XRD).

2.5. Batch adsorption experiments

Fifty milligrams of adsorbent was kept in 100 mL of 1.2×10^{-4} mol/L metal ion solutions at 25 ± 1°C for 5 h, with intermittent shaking to reach equilibrium. The solution was then filtered, and metal ions were determined using inductively coupled plasma. Blank solutions were prepared without adsorbent, having the same concentration of metal ions. This solution

was treated in the same way as above. The distribution coefficients (K_d) value was calculated by the following equation (Eq. (1)):

$$K_d = \left[\frac{I-F}{F}\right]\frac{V}{M} \quad (1)$$

where I and F are the initial and final concentration (mg/L) of metal ions in the solution phase, V is volume of initial solution in mL, and M is the dry mass of the adsorbent in g. Standard deviation for K_d value was checked by two determinations and was less than 10%.

The capacity of adsorbents for K^+ in aqueous solutions was determined by batch equilibration of 0.5 g of nanofibers, and 50 mL of 0.05 M of the KCl solution in a shaker water bath adjusted at 25 ± 1˚C until equilibration was achieved. After equilibration, the phases were separated and K^+ concentration was determined by atomic absorption spectroscopy analysis. Capacity (meq/g) was calculated from Eq. (2):

$$\text{Capacity} = C_0.Z \cdot \frac{\%\text{Uptake}}{100} \cdot \frac{V}{m}\text{meq/g} \quad (2)$$

where

$$\%\text{Uptake} = (A_{\text{eq}}/A_{\circ}) \times 100$$

C_0 is the initial concentration of solution (g/l), V is the solution volume (mL), m is the weight of the exchanger (g), and Z is the charge of the metal ion adsorbed. A_0 and A_{eq} are the initial amount of metal ions in the solution and the amount of metal ions adsorbed by adsorbent at equilibrium (g/l), respectively.

3. Results and discussion

3.1. Preparation and characterization of adsorbent

3.1.1. Synthesis of TiO_2 nanoparticles

In this work, TiO_2 nanoparticles were synthesized by hydrolysis of TTIP using OLEA as surfactant. As mentioned by [18], the hydrolysis of the titanium precursor occurs upon the reaction with water released slowly upon esterification of OLEA and EG in the presence of trimethylamine as a catalyst.

The XRD pattern of TiO_2 nanoparticles is shown in Fig. 1. The XRD pattern shows a pure rutile phase without other titanium oxide polymorphs. Average size of the obtained TiO_2 particle shown in Figs. 2 and 3 is 70 nm.

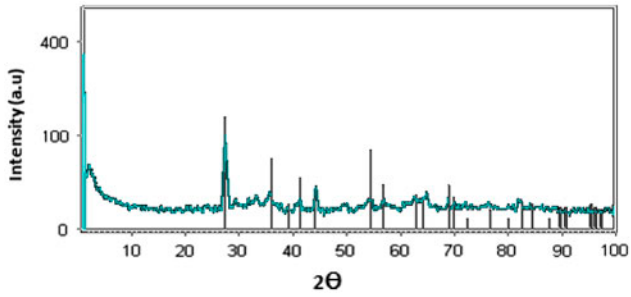

Fig. 1. XRD patterns of TiO_2 particles prepared by wet chemical method.

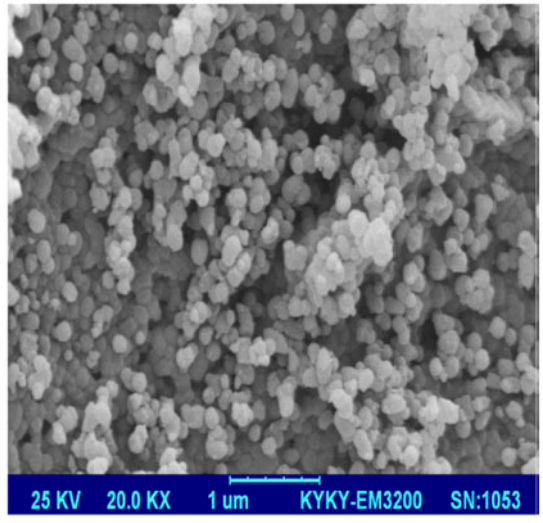

Fig. 2. SEM images of spherical TiO_2 nanoparticles.

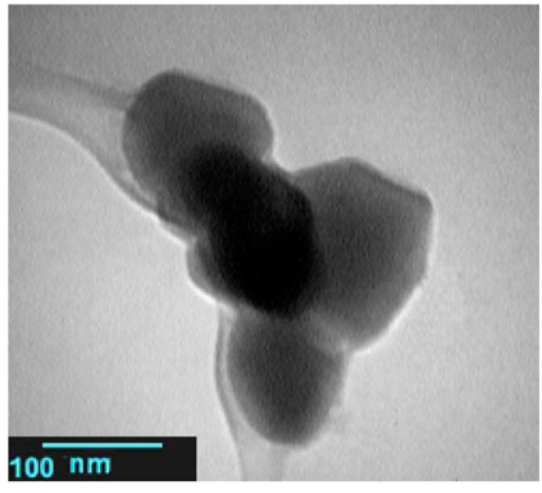

Fig. 3. Transmission electron micrographs of TiO_2 nanoparticles.

3.1.2. Synthesis of PAN/TiO_2 nanofibers

We employed a process to synthesize organic-capped TiO_2 nanoparticles. The nanoparticles prepared under these conditions were soluble in organic solvents such as DMF after extraction procedures. The extracted nanoparticles were added to the polymer dissolved in DMF and electrospun.

Fig. 4 shows the SEM image of electrospun PAN/TiO_2 nanofibers. Distribution of TiO_2 along the fiber direction and on the fiber cross section can be easily detected (Figs. 4 and 5). The diameter of fibers is in the range of 1–2 μm.

The incorporation of the TiO_2 was confirmed by comparison between Fourier Transform Infrared (FTIR) spectra of TiO_2 and PAN/TiO_2 Fig. 6(a) and (b). The absorption peaks were observed at 2,924, 2,848, and 2,960/cm correspond to the C–H stretching vibrations of the alkyl chain. A peak exhibited at 3,418/cm as a result of the C–H stretching signals in the TiO_2 samples which overlapped with an O–H band of titanol groups or adsorbed H_2O. A weak band occurred at 3,008/cm is associated to the olefinic C–H stretching. Two typical bands obtained at 1,563 and 1,426/cm of carboxylate anions of OLEA-capped TiO_2 nanoparticles. Vibrations occurred below 950/cm represents the stretching of Ti–O in the Ti–O–Ti groups [18].

The FTIR spectra of PAN/TiO_2 nanofibers showed all the characteristic bands of the functional groups of PAN with additional peaks due to TiO_2 in Fig. 6(b).

The main characteristic bands of PAN are because of C≡N (2238/cm), C=O (1728/cm), and C–O–C (1075/cm) groups. C=O and C–O–C bands come from methylacrylate comonomer [19]. These results confirm to the presence of PAN and TiO_2 nanoparticles in nanofibers.

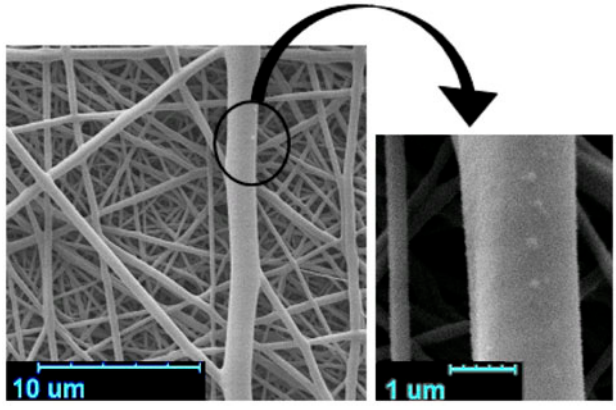

Fig. 4. SEM images of electrospun fibers of PAN/TiO_2 nanoparticles.

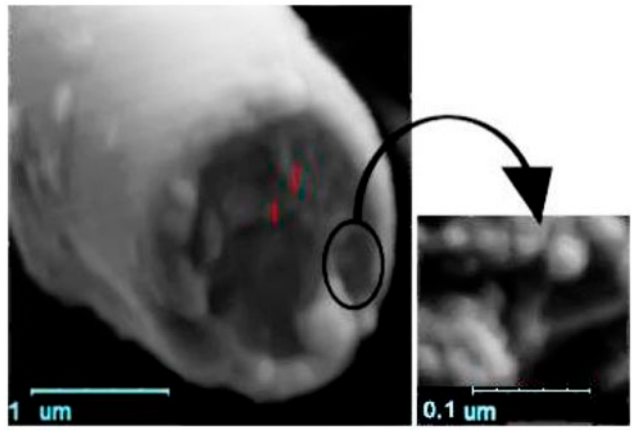

Fig. 5. SEM observation of TiO_2 nanoparticles on/into PAN nanofiber.

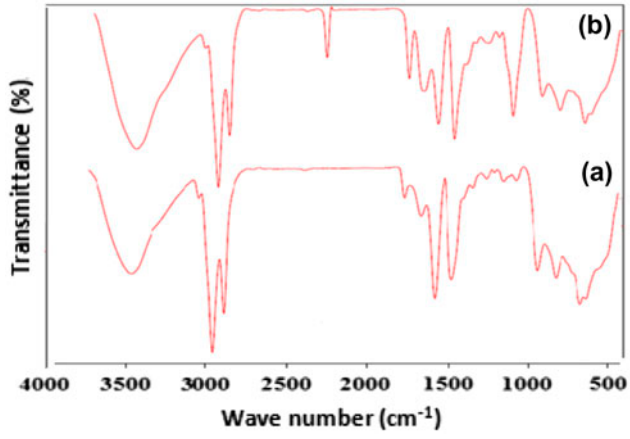

Fig. 6. FTIR spectra in the 4,000–400/cm region of (a) as-prepared OLEA-capped TiO_2 nanoparticles and (b) PAN/TiO_2 nanofibers.

The thermal degradation of prepared nanofibers was performed with heating rate of 10°C/min in air atmosphere (Fig. 7). The thermogravimetric analysis curve shows a weight loss at two stages. The weight loss of the first stage ranging between 330 and 360°C could be attributed to the cyclization reaction of PAN. The second stage of weight loss starts at about 610°C and continues up to 650°C due to the degradation of PAN chains. This figure shows that TiO_2 nanoparticles are very stable in air and no decomposition takes place in the range of 20–800°C.

3.2. Adsorption studies

The prepared materials were then used as adsorbent in removal of lead ions in aqueous solution. To

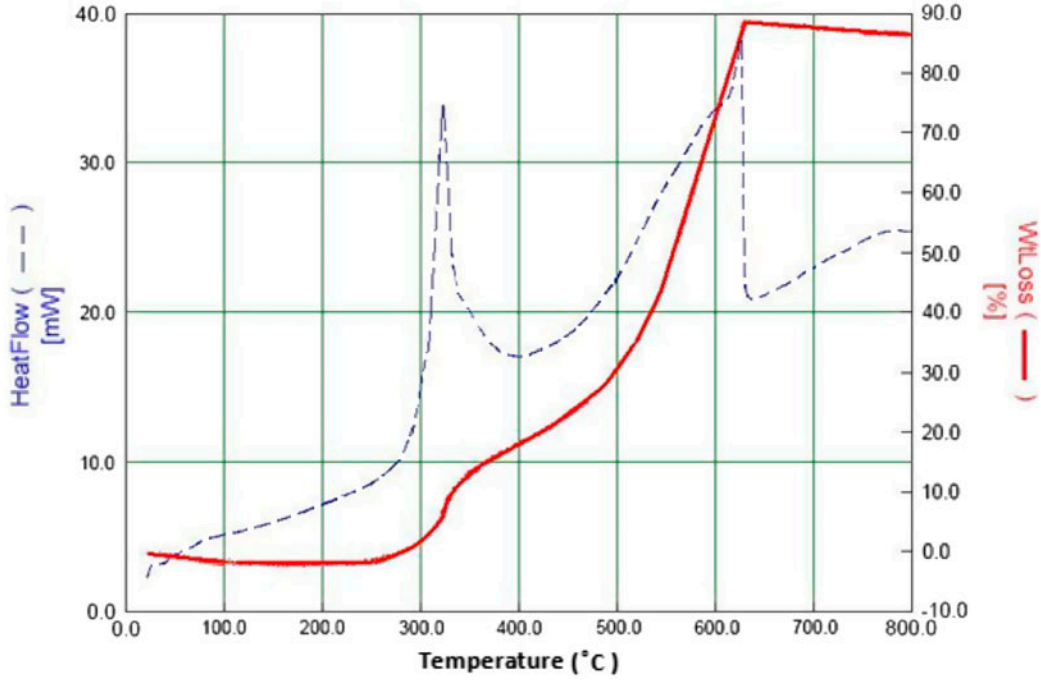

Fig. 7. Typical thermogravimetric diagram for PAN/TiO_2 nanofibers.

optimize the adsorption system, the effects of various parameters such as adsorbent type and dose, temperature, pH, concentration, and time on the adsorption of lead ions (as a model reaction) were studied.

3.2.1. Effect of adsorbent types

The capacity of three types of adsorbent (PAN powder, PAN fibers, and PAN/TiO_2 nanofibers) was studied for K^+. The results are given in Table 1. As shown in Table 1, making PAN fibers from PAN precursor plays an important role in adsorption behavior. When the batch studies were conducted with PAN powder, a poor adsorption of the K^+ ions was obtained, while using the PAN as fibers led to higher adsorption. This observation can be explained by considering the large specific surface area of nanofibers which leads to high adsorption rate and capacity.

Table 1
Capacity of synthesized adsorbents for K^+ ions

Adsorbent	Capacity (meq/g)
PAN powder	0.48
PAN fiber	0.79
10% PAN + 0.3% TiO_2	1.15
10% PAN + 1% TiO_2	1.69

To investigate the effect of TiO_2 nanoparticles, we carried out the comparative experiments with some PAN fibers loaded with different amount of TiO_2 nanoparticles (0.3 and 1%). The comparative results are summarized in Table 1. Loading a small amount of TiO_2 nanoparticles 1%) into the PAN fibers results the considerable enhancement in the adsorption capacity. Increase in TiO_2 nanoparticles loading results in increasing the adsorption capacity of nanofibers. Working with higher amounts of TiO_2 was not possible, because more than 1% TiO_2 cannot be well dispersed in DMF.

This observation can be explained by considering the surface morphology of pure PAN nanofibers and PAN/TiO_2 nanofibers (Fig. 8(a)–(c)). According to the SEM analysis, the average diameter of the electrospun PAN composite nanofibers with 0.3% TiO_2 slightly decreased compared with pure PAN nanofibers (Fig. 8(b)). When the amount of TiO_2 increased to 1% (Fig. 8(c)), the average diameter of the composite nanofibers was further decreased and the beaded structures of the nanofibers were also formed, which could be attributed to the aggregation of the TiO_2 nanoparticles. All fibers kept their fibrous shape, but became more densely packed and relaxed as the amount of TiO_2 increased.

The nanofibers with smaller diameters tend to stick together. And so the pores generated by the

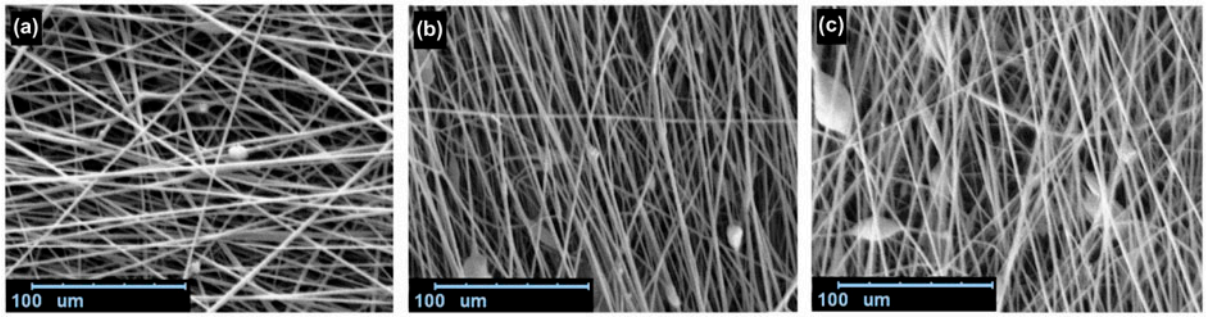

Fig. 8. SEM images of (a) PAN fibers, (b) 10% PAN modified by 0.3% TiO_2, and (c) 10% PAN modified by 1% TiO_2.

nanofibers intertwining together became smaller [20]. The reduction in nanofiber diameter results in larger specific surface area and consequently higher adsorption rate.

3.2.2. Effect of adsorbent dosage

Adsorbent dosage is one of the important parameters in adsorption processes because it determines the capacity of an adsorbent for a given initial concentration of the adsorbate under a given set of operating conditions. To achieve this aim, a series of batch experiments were conducted with the adsorbent dose of 0.5–6 g/L of the test solution.

Fig. 9 shows the effect of adsorbent dosage on the adsorption of lead ions. Increasing the adsorbent dosage causes the higher metal ions removal. A maximum removal of 97% of lead ions was obtained at 5 g/L of the adsorbent. It can be seen from Fig. 9 that an adsorbent dose of 5 g/L is sufficient for optimal removal of metal ions in aqueous solutions. A further increase in the quantity of adsorbent dose will not have any significant effect on the removal of metal ions from the solution. The initial increment in adsorption capacity with increase in adsorbent dosage was expected because as the adsorbent dose increases the number of adsorbent particles increases, thus more surface areas were available for metals attachment [21].

3.2.3. Effect of contact time

The effect of time on the removal of lead ions by PAN/TiO_2 nanofibers was studied. Fig. 10 presents the removal of lead ions with contact time. It is clear that the removal efficiency of lead ions reached a maximum value after 5 h, and no further significant increase was observed for more contact time. This may be due to the fact that initially all adsorbent sites were vacant, and the solute concentration gradient was high. Therefore based on these results, a contact time of 5 h was selected in subsequent studies.

3.2.4. Effect of pH on adsorption

The pH of the solution has been reported as an important factor in adsorption processes [22]. The variations in adsorption capacity of PAN/TiO_2

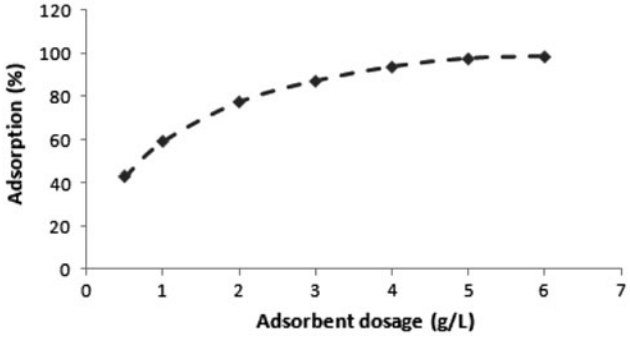

Fig. 9. Effect of adsorbent dose on adsorption of Pb^{2+} onto adsorbent.

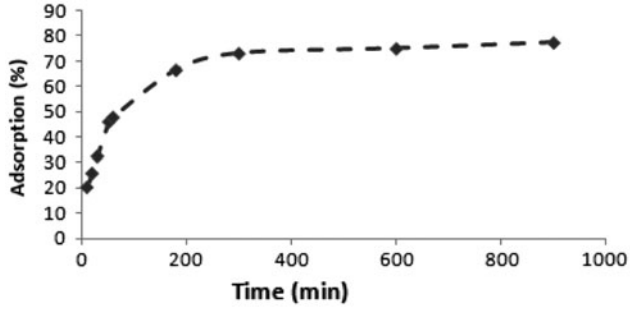

Fig. 10. Effect of contact time on adsorption of Pb^{2+} onto adsorbent.

nanofibers with increasing pH are shown in Fig. 11. It could be inferred that the adsorption capacity increased sharply as solution pH increased from 3.5–5.5.

At low pH, because of high protons concentration, positive charge density on the adsorbent increases and lead ions are fended off. pH increasing causes higher negative charge density on the adsorbent, so cation adsorption enhances due to deprotonation of cations. The maximum adsorption occurs at the pH 5.5. Probably partial hydrolysis of metal ions causes consequent reduction in adsorption capacity. Above pH 5.5, lead ions precipitated, and experiments were not get done at higher pH values [23].

3.2.5. Effect of temperature

The adsorption of metal ions was carried out at different temperatures 10, 25, 30, 40, 60, and 70°C using PAN/TiO_2 nanofibers as adsorbent. The experimental results showed that the adsorption increases with increase of solution temperature. This indicates that the adsorption of lead ions on the adsorbent is an endothermic process (Fig. 12).

By considering this result, and the two outcomes of the last section, optimum operational condition was figured to be as follows: temperature = 60°C, contact time = 5 h, and pH 5.5. Under the optimized conditions, the distribution coefficient of the lead ions on this adsorbent (K_d = 5418.15 mL/g) show good affinity of this material for Pb(II) cations in water.

3.2.6. Desorption of metal ions from nanofibers

In order to know applicability of extracting lead ions from the metal-loaded PAN/TiO_2 nanofibers and recycling the metals and adsorbent, the desorption of metal ions from the metal-loaded PAN/TiO_2 nanofibers was investigated. For this purpose, after completion of the batch adsorption experiments, the adsorbent is washed with distilled water for 24 h to ensure complete desorption, dried in a vacuum oven at 60°C, and subjected to a second run of the batch adsorption process with the same concentration of metal ions. The distribution coefficient of the first and second experiments was not changed significantly. This might be due to the ignorable amount of adsorbent lost during the adsorption–desorption process. These results strongly suggest that the PAN/TiO_2 nanofibers have a great potential as a filter for recycling metals.

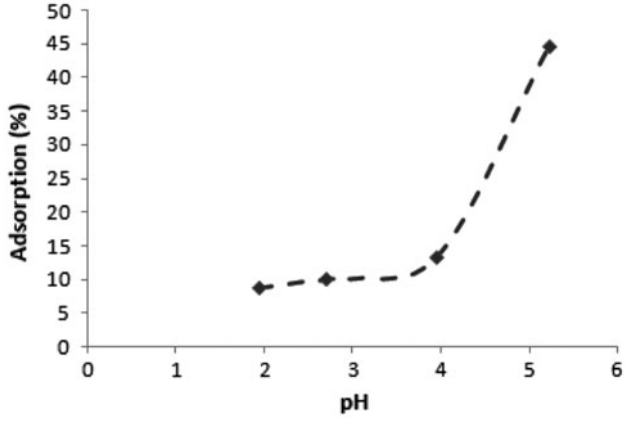

Fig. 11. Effect of pH on adsorption of Pb^{2+} onto adsorbent.

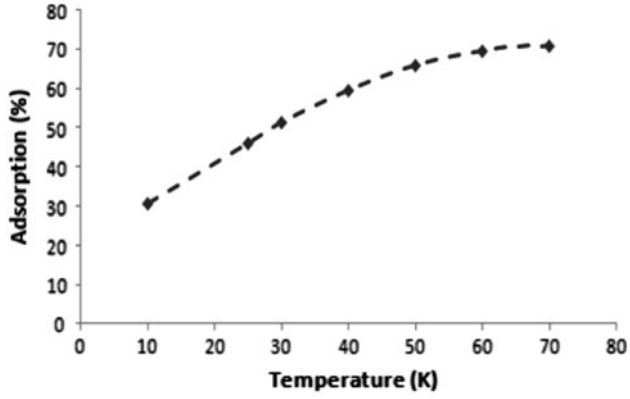

Fig. 12. Effect of temperature on adsorption of Pb^{2+} onto adsorbent.

3.2.7. Adsorption isotherm

The adsorption of Pb(II) from water by PAN/TiO_2 nanofibers assumed to have a behavior fitting with the isothermal adsorption model, that is, the adsorbate keeps a dynamic equilibrium between the adsorption and desorption at a fixed temperature.

Langmuir sorption isotherm models the monolayer coverage of the sorption surfaces and assumes that sorption occurs on a structurally homogeneous adsorbent and all the sorption sites are energetically identical (Fig. 13). The linearized form of the Langmuir equation is given by Eq. (3):

$$\frac{C_e}{q_e} = \frac{1}{Q^{\circ}b} + \frac{1}{Q^{\circ}}C_e \tag{3}$$

where q_e (in mg/g) is the adsorbate amount adsorbed by 1 g of adsorbent, C_e (in mg/L) is the

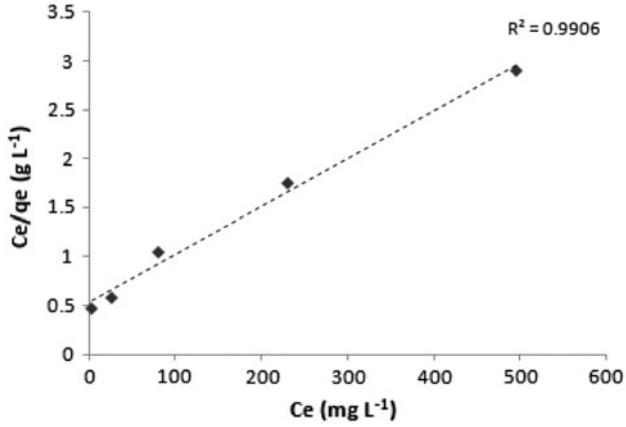

Fig. 13. Langmuir plot for the adsorption of lead(II) ions onto adsorbent.

equilibrium concentration of adsorbate in the solution, Q^o is the monolayer adsorption capacity (mg/g), and b is the constant related to the adsorption intensity. The maximum adsorption capacity (q_{max}) of adsorbent calculated from Langmuir isotherm equation is 204.08 mg/g, and the amount of b is 0.0092 (L/mg).

3.2.8. Thermodynamic parameters

In order to evaluate thermodynamic parameters of Pb(II) ions adsorption on PAN/TiO_2 fibers, the plot of $\ln(K_c)$ as a function of $1/T$ was detected (Fig. 14). From the slope and intercept of the plot and using the following equation ΔH° and ΔS° can be evaluated (Eq. (4)):

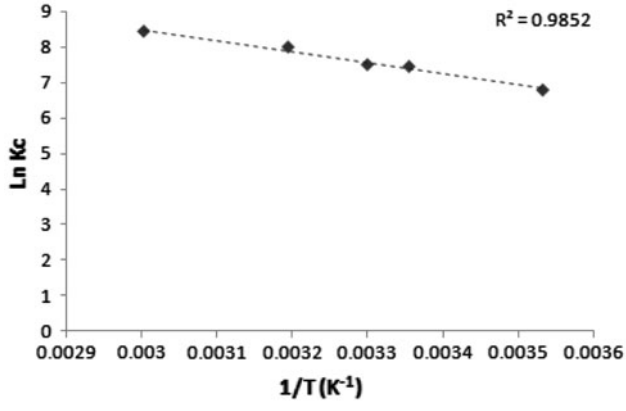

Fig. 14. Van't Hoff plot for adsorption of lead(II) ions onto adsorbent.

$$\mathrm{Ln}(K_c) = \frac{\Delta S^\circ}{R} - \frac{\Delta H^\circ}{RT} \tag{4}$$

free energy of adsorption can be calculated by following equation:

$$\Delta G^0 = \Delta H^\circ - T\Delta S^\circ \tag{5}$$

The thermodynamic results are incorporated in Table 2. The negative value of overall free energy changes indicates that the process is spontaneous, and the positive value of the enthalpy change corresponds to an endothermic adsorption of lead(II) on PAN/TiO_2 fibers. The positive value of entropy change illustrates the increased randomness at the solid/solution interface, and maybe, it reflects considerable changes occur in the structure of the adsorbent during the adsorption process [24,25].

3.2.9. Adsorption kinetics

In order to analyze adsorption kinetics of Pb(II) cations, experimental data were compared with first-order kinetic model. The model demonstrates an excellent description of kinetics behavior of the sorption process (Fig. 15). The rate constant of adsorption determined by pseudo-first-order kinetic expression (Eq. (6)):

$$\log(q_e - q_t) = \log(q_e) - \left(\frac{k_1}{2.303}\right)t \tag{6}$$

where k_1 (min^{-1}) is the first-order kinetic rate constant, q_t and q_e (mg/g) are lead uptakes at time t (min) and at equilibrium, respectively. The results of kinetic parameters are tabulated in Table 3.

Table 2
Thermodynamic parameters for the adsorption of Pb(II) ions by PAN/TiO_2 nanofibers

ΔH° (kJ/mol) = 26.21 ΔS° (kJ/mol K) = 0.149 T (K)	ΔG° (KJ/mol K)
283	−15.96
298	−18.21
303	−18.95
313	−20.44
333	−23.42

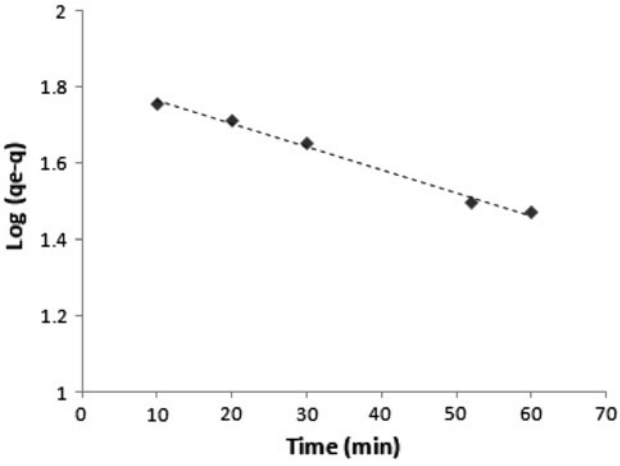

Fig. 15. Pseudo-first-order kinetic plots for the adsorption of lead(II) ions on PAN/TiO_2 nanofibers.

Table 3
Kinetic parameters for the adsorption of lead(II) ions onto PAN/TiO_2 nanofibers

C_0 (mg/L)	k_1 (min^{-1})	q_e (mg/g)	R^2
50	0.0138	66.71	0.9926

4. Conclusion

In this study, PAN/TiO_2 nanofibers were prepared through ES process and were investigated as an adsorbent in the elimination of lead(II) ions in aqueous solutions.

As a result of investigation of effective parameters, the optimum conditions achieve at pH 5.5 and time = 5 h. Contact time takes 15 h to get equilibrium. The adsorption enhances with increasing adsorbent doses. The adsorption was well described by the Langmuir adsorption isotherm model. The thermodynamic parameters indicate spontaneous ($\Delta G^\circ < 0$) and endothermic ($\Delta H^\circ > 0$) process. The pseudo-first-order kinetic model describes the dynamic behavior for the adsorption of lead(II) ions onto PAN/TiO_2 nanofibers at a range of temperatures.

References

[1] B. Gao, Y. Gao, Y. Li, Preparation and chelation adsorption property of composite chelating material poly(amidoxime)/SiO_2 towards heavy metal ions, Chem. Eng. J. 158 (2010) 542–549.
[2] A.W. Mohammad, R. Othaman, N. Hilal, Potential use of nanofiltration membranes in treatment of industrial wastewater from Ni-P electroless plating, Desalination 168 (2004) 241–252.
[3] A.S. Özcan, Ö. GÖk, A. Özcan, Adsorption of lead(II) ions onto 8-hydroxy quinoline-immobilized bentonite, J. Hazard. Mater. 161 (2009) 499–509.
[4] C.J. Buchko, L.C. Chen, Y. Shen, D.C. Martin, Processing and microstructural characterization of porous biocompatible protein polymer thin films, Polymer 40 (1999) 7397–7407.
[5] E.-R. Kenawy, G.L. Bowlin, K. Mansfield, J. Layman, D.G. Simpson, E.H. Sanders, G.E. Wnek, Release of tetracycline hydrochloride from electrospun poly(ethylene-*co*-vinylacetate), poly(lactic acid), and a blend, J. Controlled. Release 81 (2002) 57–64.
[6] Y. Sang, F. Li, Q. Gu, C. Liang, J. Chen, Heavy metal-contaminated groundwater treatment by a novel nanofiber membrane, Desalination 223 (2008) 349–360.
[7] Y. Sang, Q. Gu, T. Sun, F. Li, C. Liang, Filtration by a novel nanofiber membrane and alumina adsorption to remove copper(II) from groundwater, J. Hazard. Mater. 153 (2008) 860–866.
[8] P. Gibson, H. Schreuder-Gibson, D. Rivin, Transport properties of porous membranes based on electrospun nanofibers, Colloid. Surf. A 187–188 (2001) 469–481.
[9] G. Moroi, D. Bilba, N. Balba, Thermal behavior of palladium complexing polyacrylamidoxime polymer, Polym. Degrad. Stab. 72 (2001) 525–535.
[10] G. Moroi, D. Bilba, N. Balba, Thermal degradation of mercury chelated polyacrylamidoxime, Polym. Degrad. Stab. 84 (2004) 207–214.
[11] S. Deng, R. Bai, J.P. Chen, Behaviors and mechanisms of copper adsorption on hydrolyzed polyacrylonitrile fibers, J. Colloid. Interface. Sci. 260 (2003) 265–272.
[12] X. Zong, K.S. Kim, D. Fang, S. Ran, B.S. Hsiao, B. Chu, Structure and process relationship of electrospun bioabsorbable nanofiber membranes, Polymer 43 (2002) 4403–4412.
[13] K. Ma, C.K. Chan, S. Liao, Y.K. William, Q. Feng, S. Ramakrishna, Electrospun nanofiber scaffolds for rapid and rich capture of bone marrow-derived hematopoietic stem cells, Biomaterials 29 (2008) 2906–2103.
[14] R. Gopal, S. Kaur, C.Y. Feng, C. Chan, S. Ramakrishna, Electrospun nanofibrous polysulfone membranes as pre-filters: Particulate removal, J. Membr. Sci. 289 (2007) 210–219.
[15] F. Sayilkan, H. Sayilkan, New Adsorbents from Ti (OPr*n*)4 by the sol–gel process: Synthesis, characterization and application for removing some heavy metal ions from aqueous solution, Turk. J. Chem. 28 (2004) 27–38.
[16] S.H. Wu, X.-H. Qin, Effects of the stabilization temperature on the structure and properties of polyacrylonitrile-based stabilized electrospun nanofiber microyarns, J. Therm. Anal. Calorim. 116 (2014) 303–308.
[17] Available from: www.acq.osd.mil/.../pan_carbon_fiber_report_to_congress_10-2005.pdf.
[18] P.D. Cozzoli, A. Kornowski, H. Weller, Low-temperature synthesis of soluble and processable organic-capped anatase TiO_2 nanorods, J. Am. Chem. Soc. 125 (2003) 14539–14548.
[19] K. Saeed, S. Haider, T. Oh, S. Park, Preparation of amidoxime-modified polyacrylonitrile (PAN-oxime) nanofibers and their applications to metal ions adsorption, J. Membr. Sci. 322 (2008) 400–405.
[20] Q. Wang, D. Gao, C. Gao, Q. Wei, Y. Cai, J. Xu, X. Liu, Y. Xu, Removal of a cationic dye by adsorption/

photodegradation using electrospun PAN/O-MMT composite nanofibrous membranes coated with TiO_2, Int. J. Photoenergy. 2012 (2012) 1–8.
[21] J. Acharya, J.N. Sahu, C.R. Mohanty, B.C. Meikap, Removal of lead (II) from wastewater by activated carbon developed from Tamarind wood by zinc chloride activation, Chem. Eng. J. 149 (2009) 249–262.
[22] B.A.M. Al-Rashdi, D.J. Johnson, N. Hilal, Removal of heavy metal ions by nanofiltration, Desalination 315 (2013) 2–17.
[23] M.S. Alhakawati, C.J. Banks, Removal of copper from aqueous solution by Ascophyllum nodosum immobilised in hydrophilic polyurethane foam, J. Environ. Manage. 72(4) (2004) 195–204.
[24] A.S. Özcan, A. Özcan, Adsorption of acid dyes from aqueous solutions onto acid-activated bentonite, J. Colloid. Interface. Sci. 276(1) (2004) 39–46.
[25] S.K. Srivastava, V.K. Gupta, D. Mohan, Removal of lead and chromium by activated slag-A blast-furnace waste, J. Environ. Eng. 123 (1997) 461–468.